TELKOMNIKA, Vol.17, No.3, June 2019, pp.1118~1127
ISSN: 1693-6930, accredited First Grade by Kemenristekdikti, Decree No: 21/E/KPT/2018
DOI: 10.12928/TELKOMNIKA.v17i3.10782

Outage probability based on telecommunication range for multi-hop HALE UAVs

Mohammadreza Tarihi[1], Mohammad Mahdinejad Noori*[2], Mohammadhossein Madani[3]
Malek Ashtar University of Thechnology (MUT), Tehran, Iran,
tel: (+98)9123392339, (+98)2122945141, (+98)2122935341
*Corresponding authors, e-mail: mahdinejad@mut.ac.ir[2], mh_madani@aut.ac.ir[3]

Abstract

Cooperative relaying increases telecommunication range, improves the connectivity, and increases the reliability of data transmission; however, the transmitted power does not change. This paper analyzes the extended telecommunication range of a multi-hop cascaded network comprising N–cooperative relaying high-altitude long endurance (HALE) unmanned aerial vehicles (UAVs) under ambient conditions. A notable ambient condition is rain, which causes signals to scatter in different directions; hence, one should model the communication channel for HALE UAV as a Rayleigh channel. This paper proposes a statistical model that is based on the effect of the telecommunication range on the outage probability in an N-Rayleigh fading channel. The simulation results show that as the telecommunication range increases, the outage probability (P_{outage}) also increases, whereas when both the telecommunication range and the number of relays increase, P_{outage} decreases. An issue that has been highlighted in this paper is that, by increasing number of relays from N=1 to N=5 the telecommunication range increases and P_{outage} about 40% decreases. Moreover, in rainy conditions and with a fixed number of relays, when both the intensity of rainfall and telecommunication range increases, P_{outage} increases. For example by increasing rate of rain (R_r) from 1mm/h to 100 mm/h, P_{outage} increases around 30% in 100 Km with two relays.

Keywords: *cooperative relaying, HALE (high altitude long endurance) , N-Rayleigh fading channel, outage probability, telecommunication range, UAVs (unmanned aerial vehicles)*

1. Introduction

High-altitude long endurance unmanned aerial vehicles (HALE UAVs) are strategic UAVs that fly at altitudes ranging between 17 and 22 km above the ground in the stratosphere, have an a maximum flight time of more than 24 h, and have a range of approximately 300 km. They are in general preferred for providing reliable and stable wireless coverage for very large geographic areas. During the past few decades, whether as an ad–hoc network or alone, not only are these UAVs used for military but also for commercial applications. They are able to perform various missions such as communication relaying, control guidance, remote sensing, navigation, surveillance and others [1-4].

In recent years, multifarious papers have reported UAVs as aerial platform communications is expected to an important role in the future communication systems. For wide coverage, extended telecommunication range with a relay, information dissemination, data collection, and other use cases, UAV-aided wireless communication can be used [5-7]. Accordingly, the performance of the UAV's network in different layers has been studied in numerous papers. In [8-10], research on network media access control (MAC) layer algorithms and routing protocols were performed. In [11-14], an optimal relaying plan based on the UAV's flight path and flight parameters was reported. In [15, 16], the network performance was investigated using techniques such as multiple-input multiple-output (MIMO) systems, as well as antenna beam forming (BF). In [15-17], the strategy of cooperative relaying UAVs was employed, and both the capacity and the probability of errors in single-input single-output (SISO) and MIMO scenarios were analyzed. In [18], a statistical model based on the coverage of the outage probability in a compound fading channel (Lognormal-Nakagami) for MANET networks was investigated. In [19], coverage of signals for a high altitude platform (HAP) relay in a 3G communications network was investigated, and in [20], both line-of-sight (LoS) and non-LoS (NLoS) channels were analyzed for cellular systems.

Received August 7, 2018; Revised February 17, 2019; Accepted March 15, 2019

The results of all previous studies, prove that the performance of the UAVs relay network is directly dependent on the propagation of relay signals. Therefore, in order to extend the telecommunication range, this study uses a multi-hop cascaded network comprising N-cooperative relaying HALE UAVs, and, for the worst-case scenario, proposes a statistical model based on how the telecommunication range affects the outage probability in an N-Rayleigh fading channel.

This unique study builds on existing results by making the following contributions. Exact expressions are presented to show the outage probability based on the telecommunication range in a multi-hop N-Rayleigh fading channel. Finally, the effect of rain, which is one of the most important factors of ambient conditions on the outage probability, is considered.

The rest of this paper is organized as follows. In Section 2, the problem statement and the reason for employing a cooperative relaying scenario for extended telecommunication range in HALE UAVs is presented. Section 3 introduces the system model and channel model under rainy conditions. Then, in Section 4, the statistical model based on the outage probability and exact expressions for the outage probability based on the telecommunication range in a multi-hop N-Rayleigh fading channel, are derived. Section 5 discusses the results of computer simulations. Finally, Section 6 concludes this paper and summarizes the key findings.

2. Problem Statement

Considering the geometrical model of Figure 1, and without taking into account constraints of characteristics of LoS link, such as the transmitted power and antenna gain, the following equations describe the maximum range in HALE UAVs [18, 19]. Table 1 defines the parameters of the (1-7).

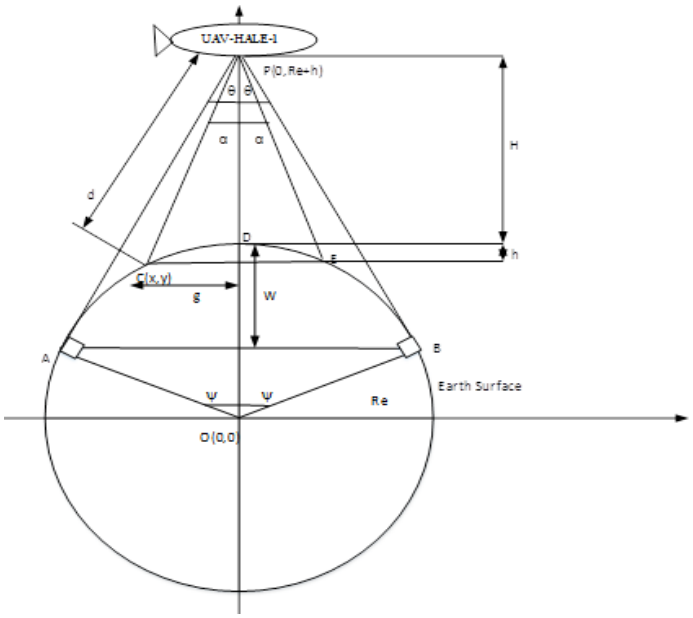

Figure 1. Geometric model of HALE UAV [16]

$$S = 2\pi Rh \tag{1}$$

$$h = \frac{d^2 - H^2}{2H + 2R} \tag{2}$$

$$\alpha = Arc\,tan\frac{g}{H + h} \tag{3}$$

$$g = \frac{\sqrt{(d^2 - H^2)(4RH + 4R^2 - d^2 + H^2)}}{2H + 2R} \tag{4}$$

$$S_{max} = 2\pi R \frac{RH}{R+H} \quad (5)$$

$$\alpha_{max} = \theta = Arc\,cos \frac{\sqrt{H^2 + 2RH}}{R+H} \quad (6)$$

$$\angle BOP = Arc\,tan \frac{\sqrt{H^2 + 2RH}}{R} \quad (7)$$

Table 1. Defined Parameters

Parameters	Description
R	Earth radius ® is about 6370 km
H	UAV height
d_{max}	Maximum propagation distance of the signal
r_{max}	Maximum coverage
S_{max}	Maximum spherical area covered
θ	Minimum antenna beam–width

By making the ∠ BOP small, the high altitude of the HALE UAV changes $\widehat{ADB}$ to a straight line and changes the crust of the sphere (i.e., CDE) to a circle with D as its center. Therefore:

$$d_{max} = \sqrt{H^2 + 2RH} \quad (8)$$

$$g = r = \sqrt{\frac{R(d^2 - H^2)}{R+H}} \quad (9)$$

$$r_{max} = \sqrt{\frac{2R^2H}{R+H}} \quad (10)$$

$$R \gg H \;\rightarrow\; r_{max} \cong\; d_{max} \;\cong \sqrt{2RH} \quad (11)$$

As depicted in Figure 2, (11) shows that the maximum telecommunication range and coverage *(d_{max}, r_{max})* is a function of the UAV altitude. Considering the typical values for a telecommunication link of HALE UAV, the maximum telecommunication range depend on the transmitted power, bit rate, required E_b/N_0 at the receiver, antenna gain, and channel noise [19].

$$d \leq \sqrt{\frac{P_{TXH} G_H G_G}{\Delta L K R_b T \gamma_0} \left(\frac{\lambda}{4\pi}\right)^2} = \sqrt{\frac{P_{TXH} G_H G_G \lambda^2}{16\pi^2 \Delta L K R_b T}} {\gamma_0}^{-1/2} \quad (12)$$

$$r \leq \sqrt{\frac{R(\frac{P_{TXH} G_H G_G \lambda^2}{16\pi^2 \Delta L K R_b T} {\gamma_0}^{-1} - H^2)}{R+H}} \quad (13)$$

from (12), the average power of the receiving signal in the ground station *(P_{RXG})* can be expressed as:

$$P_{RXG} = \frac{P_{TXH} G_H G_G}{L_f \Delta L} \quad (14)$$

where P_{TXH} is the UAV transmitter power, G_H , G_G are the transceiver antenna gains, ΔL is the atmospheric refraction loss, and $L_f = (\frac{4\pi d}{\lambda})^2$ is the free-space signal propagation path loss for the wavelength (λ). Also Figure 3 shows the variation in the maximum telecommunication range against the required E_b/N_0 at the receiver. The simulation parameters are given in Table 2.

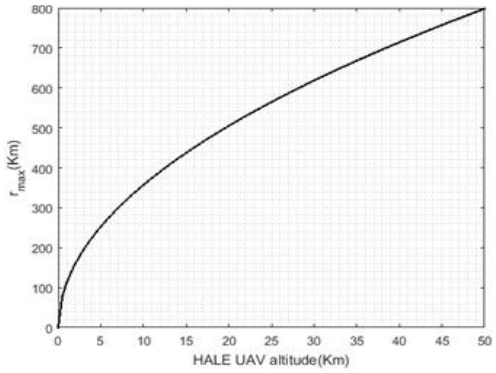

Figure 2. Variation in maximum telecommunication range and radius of coverage area with HALE UAV altitude

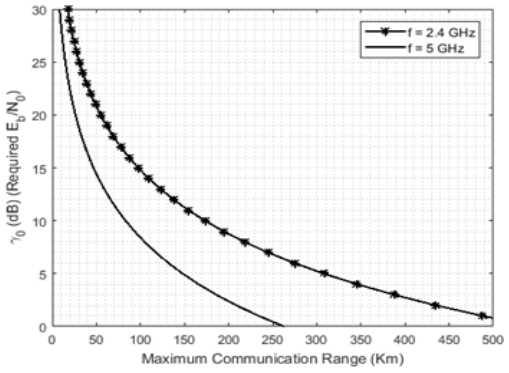

Figure 3. Maximum range versus required E_b/N_0

Table 2. Simulation Parameters

Parameter	Value	Definition
P_{TXH}	30 dBm	Power per carrier
G_H	2 dBi	Antenna gain transmitter (HALE UAV)
G_G	30 dBi	Backhaul ground station antenna gain
f	2.4 GHz	Frequency
	5 GHz	
B	25 MHz	System bandwidth
η	QPSK	Modulation type
Rb	40 Mbits/s	Bit rate

The results of the simulation in Figure 3 show that when required E_b/N_0 is reduced, the maximum telecommunication range is also reduced, especially at high frequencies. For example, the minimum required $\mathrm{E_b/N_0}$ at the receiver for QPSK modulation is 7.8 dB @ BER=10^{-6}, for which the maximum telecommunication range is about 200 and 100 km at 2.4 and 5 GHz, respectively. Therefore, for an extended telecommunication range in HALE UAVs with the same link parameters, a cooperative relaying scenario should be used. The system model and channel model of this scenario are described below.

3. HALE UAV System and Channel Model

3.1. System Model

A multi-hop cooperative relaying technology enhances the spectral efficiency and extends the coverage of both cellular and ad-hoc wireless networks [21, 22]. In cascade cooperative multi-hop relaying technology, the source and destination nodes communicate through a set of cooperating relay nodes in which the transmitted signals propagate through cascaded relay nodes in order to extend coverage for improving the performance of the network. The signal received at the relay is usually processed before being forwarded to the destination. There are several signal relaying protocols such as AF and DF [23]. Figure 4 shows N–cooperative relaying HALE UAVs.

3.2. Channel Model

A HALE UAV telecommunication channel is expected to be Ricean in its general form, i.e., the Rice distribution can be employed to describe the statistics of the channel [5]; hence, the telecommunication channel model can be expressed as follows [24]:

$$h = \sqrt{\frac{K}{K+1}}h_{LOS} + \sqrt{\frac{1}{K+1}}h_{NLOS} \quad (15)$$

In (15), $\mathrm{h_{LOS}}$ is the free-space LoS response and $\mathrm{h_{NLOS}}$ is the response due to the scattered waves (NLoS). K is the Ricean factor, and expresses the relative power of the direct and scattered components of the received signal, and provides an indication of the link quality. In the case of $K = 0$, a Rayleigh distribution describes the channel, whereas a very large value of K, i.e., $K \to \infty$, implies the presence of a Gaussian channel.

Moreover, the rain is confined to the first 2.5–5 km of the atmosphere depending on the latitude [25]. Hence, an EM wave propagating in the troposphere is directly affected by rain. An important conclusion of this explanation is that multipath signals are observed, even in unobstructed LoS links during rain, but they are not observed during clear-sky conditions. Hence, the h channel can be expressed by (16):

$$h = \sqrt{\frac{K_r}{K_r+1}}h_{LOS} + \sqrt{\frac{1}{K_r+1}}h^r_{NLOS} \quad (16)$$

In (16), h_{LOS} is a deterministic, non-fading LoS response, and H^r_{NLOS} is a stochastic response of the scattered waves owing to rain. K_r is the Ricean factor, and directly refers to the rainy conditions. In a heavy rainfall environment, $K_r \to 0$ and channel h is approximately equal to h^r_{NLOS}. In this situation, the channel h is modelled Rayleigh fading. Empirically, the Ricean factor ($K_{r)}$ is given as [26, 27]

$$K_r(dB) = \begin{cases} 16.88\text{-}0.04\mathrm{R_r}\ dB & R_r \neq 0 \\ \infty\ dB & R_r = 0 \end{cases} \quad (17)$$

This empirical relationship between the Ricean factor $\mathrm{K_r}$ (in dB) and the rainfall rate R_r (in mm/h) is dependent upon factors such as the elevation, frequency, polarization, climate, and environment. In the worst case, $K_r \to 0$, (R_r increase), and the channel h is described by a Rayleigh distribution. Rain primarily contributes to signal attenuation, and the rain attenuation $\mathrm{L_r}$ is empirically obtained by using the specific rain attenuation $\mathrm{L_r}$ (dB/km) [28, 29], which is defined as (18).

$$\begin{aligned} &L_r = \gamma_r d_r \\ &\gamma_r(\tfrac{dB}{km}) = a_r R_r^{b_r} \\ &d_r = |H_r - H_R|/sin\theta \end{aligned} \quad (18)$$

In (18), $\mathrm{d_r}$ is the total rainy path length and is geometrically obtained, $\mathrm{H_r}$ is the effective rain height, $\mathrm{H_R}$ is the altitude of the HALE UAV, θ is the elevation angle of the HALE UAV platform, and the values of the empirical regression coefficients $\mathrm{a_r}$ and $\mathrm{b_r}$ depend on the climatic zone, the transmission frequency, and the polarization.

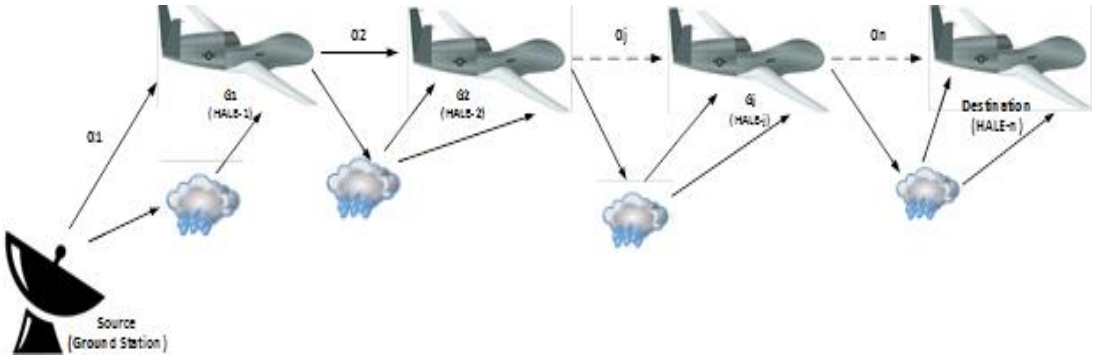

Figure 4. N-hop cooperative relaying communication

The rain attenuation is significant at frequencies above 10 GHz, where the wavelength and raindrop size (about 1.5 mm) are comparable, so the attenuation is quite large. Thus, HALE UAV-based communication systems operating in the Ka and V frequency bands are susceptible to rain; their L and S frequency-band counterparts are not susceptible to rain. Therefore, the channel model in the system model shown in Figure 4 is an N-Rayleigh channel, where its statistical model is explained below.

4. Statistical Model Based on Outage Probability

The model of attenuation for an N-Cooperative relaying HALE UAV link, as shown in Figure 4, is given as:

$$L_f = \prod_{i=1}^{N} L_i \tag{19}$$

In (19), L_f is the total signal attenuation, that is defined as an "N-Rayleigh" random variable, and L_i is the signal attenuation for each link that defines a Rayleigh distributed random variable with a probability density function (pdf) of $f_{L_i}(l_i) = \frac{l}{{\sigma_i}^2} exp(-\frac{l^2}{2{\sigma_i}^2})$ .The mth moment of L_i, i.e., $E(L_i^m)$, is $E(L_i^m) = \int_0^\infty \frac{l^{m+1}}{{\sigma_i}^2} exp\left(-\frac{l^2}{2{\sigma_i}^2}\right) dl = (2{\sigma_i}^2)^{\frac{m}{2}} \Gamma(\frac{m}{2}+1)$, where the gamma function is defined as $\Gamma(x) = \int_0^\infty t^{x-1}e^{-t}dt$. The density and distribution functions of L_f in terms of the Meijer G-function [30] are:

$$f_{L_f}(l_f) = 2(2^N\sigma^2)^{-\frac{1}{2}} G_{0,N}^{N,0}\left((2^N\sigma^2)^{-1}{l_f}^2 \middle| \frac{1}{2}, \cdots, \frac{1}{2}\right) \tag{20}$$

$$F_{L_f}(l_f) = 2(2^N\sigma^2)^{-\frac{1}{2}} l_f\, G_{1,N+1}^{N,1}\left((2^N\sigma^2)^{-1}{l_f}^2 \middle| \begin{matrix} \frac{1}{2} \\ \frac{1}{2}, \cdots, \frac{1}{2}, -\frac{1}{2} \end{matrix}\right) \tag{21}$$

In (20) and (21), the Meijer G-function is a generalized hypergeometric function, and is defined using a contour integral representation:

$$G_{p,q}^{m,n}\left(z \middle| \begin{matrix} a_1, \cdots, a_p \\ b_1, \cdots, b_p \end{matrix}\right) = \frac{1}{2\pi j} \oint \frac{\prod_{i=1}^{m} \Gamma(b_i + s) \prod_{i=1}^{n} \Gamma(1 - a_i - s)}{\prod_{i=n+1}^{p} \Gamma(a_i + s) \prod_{i=m+1}^{q} \Gamma(1 - b_i - s)}\, z^{-s}\, ds \tag{22}$$

in (22), z, $\{a_i\}_{i=1}^{p}$ and $\{b_i\}_{i=1}^{q}$ are complex-valued, and contour ¢ is chosen so that it separates the poles of the gamma product in the numerator. The mth moment of L_f is given by $v_m = (2^N\sigma^2)^{\frac{m}{2}}\left[\Gamma\left(\frac{m}{2}+1\right)\right]^N$ where $\sigma^2 = \prod_{i=1}^{N} \sigma_i^2$. However, the outage probability is defined as the probability that the received instantaneous SNR on the destination is lower than the SNR threshold. In other words,

$$P_{outage} = \int_0^{\gamma_{req.}} f_\gamma(\gamma) d\gamma \tag{23}$$

where $f_\gamma(\gamma)$ is the distribution of the instantaneous received SNR. The attenuation in the channel corresponding to the SNR threshold is $l_f = {}^{A}/_{\gamma_{eq}}$ (from (12)), where the constant A is equal with ${}^{P_t G_t \dots G_r}/_{KT\Delta LR_b}$. Given the relationship l_f and γ_{eq} and use of following lemma: Lemma 1: To compute the cumulative distribution of Y = g(X) in terms of the cumulative distribution of X, note that

$$F_Y(y) = P(Y \le y) = P\{g(X) \le y\} = P\{X \le g^{-1}(y)\} = F_X(g^{-1}(y)) \tag{24}$$

for g decreasing within the range of X:

$$F_Y(y) = P(Y \le y) = P\{g(X) \le y\} = P\{X \ge g^{-1}(y)\} = 1 - F_X(g^{-1}(y)) \quad (25)$$

thus, from (25) the outage probability is:

$$P_{outage} = 1 - F_{L_f}(l_f) \left| l_f = {}^{A}/_{\gamma_{req.}} \right. \quad (26)$$

Therefore, $\mathrm{F_{L_f}(d, l_f)}$ is the cumulative density function (CDF) of the N-Rayleigh distribution. By applying (21), we get:

$$\begin{aligned} &F_{L_f}(d) \left| l_f = {}^{A}/_{\gamma_{req}}, \sigma^2 = \left(\frac{4\pi d}{\lambda}\right)^2 \right. \\ &= 2\left(2^N \left(\frac{4\pi d}{\lambda}\right)^2\right)^{-\frac{1}{2}} \left(\frac{A}{\gamma_{req}}\right) G^{N,\ \ 1}_{1,N+1}\left((2^N \left(\frac{4\pi d}{\lambda}\right)^2)^{-1} (\frac{A}{\gamma_{req}})^2 \right| \begin{matrix} \frac{1}{2} \\ \frac{1}{2}, \ldots, \frac{1}{2}, -\frac{1}{2} \end{matrix} \Bigg) \end{aligned} \quad (27)$$

finally

$$\begin{aligned} &P_{outage} \\ &= 1 \\ &- F_{L_f}(l_f) \left| l_f = {}^{A}/_{\gamma_{req}} \right. \\ &= 1 \\ &- 2\left(2^N \left(\frac{4\pi d}{\lambda}\right)^2\right)^{-\frac{1}{2}} \left(\frac{A}{\gamma_{req}}\right) G^{N,\ \ 1}_{1,N+1}\left((2^N \left(\frac{4\pi d}{\lambda}\right)^2)^{-1} (\frac{A}{\gamma_{req}})^2 \right| \begin{matrix} \frac{1}{2} \\ \frac{1}{2}, \ldots, \frac{1}{2}, -\frac{1}{2} \end{matrix} \Bigg) \end{aligned} \quad (28)$$

The expansion of the $G^{N,\ \ 1}_{1,N+1}(.)$ function is difficult for different values of N, but using the references [30-33] for the values of N = 1, 2, 3, 4, 5 and the various values of the $G^{N,\ \ 1}_{1,N+1}(.)$ function are obtained. For N = 1 and N = 2, the $G^{N,\ \ 1}_{1,N+1}(.)$ function in (27) reduces to a Rayleigh and double-Rayleigh distribution, respectively. When N = 1, the following equation results are obtained: [31, (Eq. §07.34.03.0273.01)]

$$G^{1,1}_{1,2}\left(z \left| \begin{matrix} \frac{1}{2} \\ \frac{1}{2}, -\frac{1}{2} \end{matrix} \right. \right) = e^{-z} z^{\frac{1}{2}} \Gamma(0) L^1_{-1}(z) \left| z = (2\left(\frac{4\pi d}{\lambda}\right)^2)^{-1} (\frac{A}{\gamma_{eq}})^2 \right. \quad (29)$$

In (29) $\mathrm{L^{\lambda}_{\vartheta}(z)}$ is the Laguerrel function, that is, [31, (Eq. § 07.03.26.0002.01)]

$$L^{\lambda}_{\vartheta}(z) = \frac{(\lambda+1)_{\vartheta}}{\Gamma(\vartheta+1)}\ {}_1F_1(-\vartheta; \lambda; z)\ ;\ -\lambda \in N^+ \quad (30)$$

for $\vartheta = -1$ and $\lambda = 1$, (29) reduces to $\frac{\Gamma(1)}{\Gamma(0)} {}_1F_1(1;1;z)$. Moreover, for $a = 1, b = 1$, the hypergeometric function ${}_1F_1(a;b;z)$ *is:* $-\frac{1}{z}(1 - e^z)$ [31, (Eq. § 07.20.03.0026.01)]. Hence, for N=1:

$$\begin{aligned} &F_{L_f}(d) = 2\left(2^1 \left(\frac{4\pi d}{\lambda}\right)^2\right)^{-\frac{1}{2}} \left(\frac{A}{\gamma_{req}}\right)(1 - e^{-z}) \left| z = 2\left(\frac{4\pi d}{\lambda}\right)^2)^{-1} (\frac{A}{\gamma_{eq}})^2 \right., \\ &P_{outage} = 1 - F_{L_f}(d) \end{aligned} \quad (31)$$

for N=2, (20) becomes:

$$f_{L_f}(d) = 2(2^2\left(\frac{4\pi d}{\lambda}\right)^2)^{-\frac{1}{2}} G_{0,2}^{2,0}\left((2^2\left(\frac{4\pi d}{\lambda}\right)^2)^{-1}(\frac{A}{\gamma_{eq}})^2 \middle| \frac{1}{2},\frac{1}{2}\right) \quad (32)$$

from [31, (Eq. § 07.34.03.0605.01)]:

$$\begin{aligned} &G_{0,2}^{2,0}\left(z\middle|\frac{1}{2},\frac{1}{2}\right) = 2z^{\frac{1}{2}(b+c)}K_{b-c}\left(2\sqrt{z}\right)\Big|b,c=\frac{1}{2} \\ &= 2\sqrt{z}K_0\left(2\sqrt{z}\right)\Big|z=(2^2\left(\frac{4\pi d}{\lambda}\right)^2)^{-1}(\frac{A}{\gamma_{eq}})^2 \end{aligned} \quad (33)$$

in (33), $K_v(.)$ is the modified Bessel function of the second kind. Replacing G-function in (32) with (33) and integrating the result, we obtain the following equation.

$$\begin{aligned} &F_{L_f}(d) = -2\left(2^2\left(\frac{4\pi d}{\lambda}\right)^2\right)^{-\frac{1}{2}}\left(\frac{A}{\gamma_{req}}\right)2\sqrt{z}K_1(2\sqrt{z})\Big|z=(2^2\left(\frac{4\pi d}{\lambda}\right)^2)^{-1}(\frac{A}{\gamma_{eq}})^2, \\ &P_{outage} = 1 - F_{L_f}(d) \end{aligned} \quad (34)$$

applying N = 3, 4, and 5 to (27), will be achieved (35), (36), and (37), respectively:
for N=3:

$$\begin{aligned} F_{L_f}(d) = \frac{z}{2}\sum_{k=0}^{\infty}\frac{(-1)^k}{(k)!^3\,(k+1)} &\times\left[ln^2(z) - 2\,ln(z)\,C_3(k) + C_3^{(1)}(k) + [C_3(k)]^2\right]z^k\Big|z \\ &= (2^3\left(\frac{4\pi d}{\lambda}\right)^2)^{-1}(\frac{A}{\gamma_{eq}})^2 \end{aligned} \quad (35)$$

for N=4:

$$\begin{aligned} F_{L_f}(d) = \frac{z}{6}\sum_{k=0}^{\infty}&\frac{1}{(k)!^4\,(k+1)} \\ &\times\left[-ln^3(z) + 3\,ln^2(z)\,C_4(k) - 3\,ln(z)\left[C_4^{(1)}(k) + [C_4(k)]^2\right] + C_4^{(2)}(k)\right. \\ &\left. + 3C_4^{(1)}(k)C_4(k) + [C_4(k)]^3\right]z^k\Big|z = (2^4\left(\frac{4\pi d}{\lambda}\right)^2)^{-1}(\frac{A}{\gamma_{eq}})^2 \end{aligned} \quad (36)$$

for N=5:

$$\begin{aligned} F_{L_f}(d) == \frac{z}{24}\sum_{k=0}^{\infty}&\frac{(-1)^k}{(k)!^5\,(k+1)} \\ &\times\Big[ln^4(z) - 4\,ln^3(z)\,C_5(k) \\ &+ 6\,ln^2(z)\Big[C_5^{(1)}(k) \\ &+ [C_5(k)]^2\Big] - 4\,ln(z)\left[C_5^{(2)}(k) + 3C_5^{(1)}(k)C_5(k) + [C_5(k)]^3\right] + C_5^{(3)}(k) \\ &+ C_5^{(2)}(k)C_5(k) + 3\left[C_5^{(1)}(k)\right]^2 + 6[C_5(k)]^2C_5^{(1)}(k) + [C_5(k)]^4\Big]z^k\Big|z \\ &= (2^5\left(\frac{4\pi d}{\lambda}\right)^2)^{-1}(\frac{A}{\gamma_{eq}})^2 \end{aligned} \quad (37)$$

where $C_N^{(l)}(k) = B_N^{(l)}(k) + \frac{l!}{(k+1)^{l+1}}$. In addition, $B_N^{(l)}(k)$ is:

$$B_N^{(l)}(k) = N\left[\psi^{(l)}(1) + (-1)^{l+1}\left[\psi^{(l)}(1) - \psi^{(l)}(k+1)\right]\right], for\ n \geq 2 \quad (38)$$

in (38), $\psi^{(p)}(x) = \left(\frac{d^p}{x^p}\right)\psi(x) = \left(\frac{d^{p+1}}{x^{p+1}}\right)ln\,\Gamma(x)$ is the pth polygamma function. With this description, the amount of P_{Outage} for different values of N is given by (28), which is simulated and shown in Figure 5.

5. Results and Discussion

Figure 5 shows the telecommunication range with the number of cooperative relays against outage probability in a multi-hop link comprising N–cooperative relaying HALE UAVs. The simulation shows that as the telecommunication range increases, the more the outage probability (P_{outage}) increases; however when both the telecommunication range and the number of relays increase, P_{outage} decreases.

For example, for a specified telecommunication range (i.e., 100 km), the outage probability decreases from approximately 0.9 to 0.2 when the number of cooperative relays from N=1 to N=5 increases. Therefore, by the increasing number of relays in this scenario, in addition to increasing the telecommunication range, the outage probability (P_{outage}) also decreases.

Moreover, Figure 6 shows that in rainy conditions and with a fixed number of relays, whenever both the rate of rainfall and telecommunication range increases, P_{outage} increases. When the rain rate $(\mathrm{R_r})$ increases, SNR decreases; however, the effect of h_{NLOS}^{r} increases. Because of the considerable attenuation at frequencies above 10 GHz in rainy conditions, with increasing rain rate, the maximum telecommunication range of HALE UAV from the source to destination decreases yet, hence, the outage probability increases.

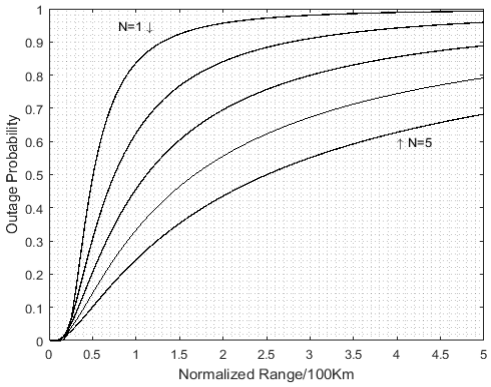

Figure 5. Extended range with number of cooperative relays versus outage probability

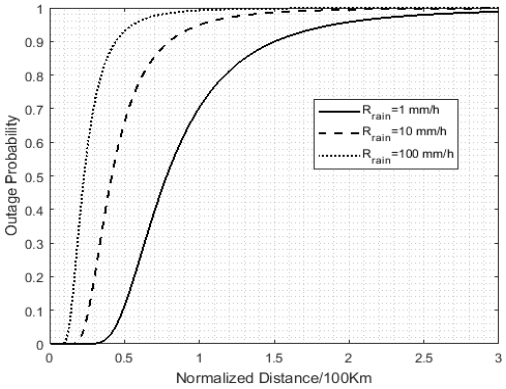

Figure 6. Outage probability based on telecommunication range under rainy conditions

6. Conclusion

UAVs as an aerial communications platform is expected to an important role in future communication systems. Increasing telecommunication range with the cooperative relaying is one of the UAV-aided wireless communication applications which discussed in this paper. Cooperative relaying simultaneously extends the range and improves the link connectivity; however, the transmitted power does not change. In this study, increasing telecommunication range for a multi-hop cascaded network comprising N–cooperative relaying HALE UAVs analyzed. We first studied the geometric model for the HALE UAV telecommunication range and showed that for increasing telecommunication range in HALE UAV with the same link parameters, especially at high frequencies, a cooperative relaying scenario should be used. Next, we proposed a system model and channel model under rainy conditions. It was shown that an N-Rayleigh fading channel will be created. Finally, we proposed a statistical model based on the effect of telecommunication range on the outage probability in an N-Rayleigh fading channel. An issue that has been highlighted in this paper is that, in the N-Rayleigh fading channel, when the telecommunication range increases, so too will the P_{outage}, whereas when both the telecommunication range and the number of relays sincreases, P_{outage} decreases significantly.

References

[1] Zeng Y, Zhang R, Lim TJ. Wireless communications with unmanned aerial vehicles: opportunities and challenges. *IEEE Communications Magazine*. 2016; 54(5): 36-42
[2] Grace D, Mohorčič M. Broadband communications via high altitude platforms. John Wiley & Sons Ltd. 2011.
[3] Valavanis KP, Vachtsevanos GJ. Handbook of Unmanned Aerial Vehicles. Springer Netherlands. 2015.

[4] Widiawan AK, Tafazolli R. High altitude platform station (HAPS): A review of new infrastructure development for future wireless communications. *Wirel. Pers. Commun*. 2007; 42(3): 387-404.
[5] Baek H, Lim J. Design of Future UAV-Relay Tactical Data Link for Reliable UAV Control and Situational Awareness. *IEEE Communications Magazine*. 2018; 56(10): 144-150.
[6] Han SI, Baek J, Han Y. *Deployment of multi-layer UAV relay system*. IEEE Wireless Communications and Networking Conference (WCNC). 2018: 15-18.
[7] Ebrahimi D, Sharafeddine S, Ho PH, Assi C. UAV-Aided Projection-Based Compressive Data Gathering in Wireless Sensor Networks. *IEEE Internet of Things Journal*. 2018: 1-1.
[8] Gu DL, Ly H, Hong X, et al. *A centralized intelligent channel assigned multiple access for multilayer ad-hoc wireless networks with UAVs*. IEEE Wirel. Commun. Conf. 2000; 879-884.
[9] Xu K, Hong X, Geral M, et al. *Landmark routing in large wireless battlefield networks using UAVs*. IEEE Mil. Commun. Conf. 2001; 1: 230-234.
[10] Perumal S, Baras JS, Graf CJ, et al. *Aerial platform placement algorithms to satsfy connectivity, capacity and survivability constraints in wireless ad-hoc networks*. IEEE Mil. Commun. Conf. 2008: 1-8.
[11] Kramer G, Gastpar M, Gupta P. Cooperative strategies and capacity theorms for relay networks. *IEEE Trans. on Inf. Theory*. 2005; 51(9): 3037-3063.
[12] Zhu H, Swindlehurat AL, Liu K. Optimization of MANET connectivity via smart deployment/movement of unmanned air vehicle. *IEEE Trans. on Veh. Technol*. 2009; 58 (7): 3533-3546.
[13] Xu ZX, Yuan J, Wang Y, et al. UAV relay network to provide communication in mobile ad-hoc networks. *J. of Tsinghua Univ.: Sci. Technol.* 2011; 51 (2): 150-155.
[14] Zhan P, Yu K, Swindlehurst Al. Wireless relay communication with unmanned aerial vehicle: performance and optimization. *IEEE Trans. on Aerosp. and Electron. Syst*. 2011; 47 (3): 2068-2085.
[15] Feihong D, Yuanzhi H, Haitao N, Zongsheng Z, Jingchao W. *System capacity analysis on constellation of interconnected HAP networks*. IEEE Fifth Int. Conf. on Big Data and Cloud Comput. 2015: 154-159.
[16] Feihong D, Min L, Xiangwu G, Hongjun L, Fengyue Gao. Diversity performance analysis on multiple HAP networks. *Sens. Net. Open Access J*. 2015.
[17] Ou YJ, Zhuang Y, Xue Y, et al. UAV relay transmission scheme and its performancer analysis over asymmetric fading channel. *Acta Aeronanutica et Astronautica Sinica*. 2013; 34(1): 130-140.
[18] Shuaike H, Yanwen L, Hao L, Quiming Z, Shengkui Z, Weizhen C, Zhicheng J. An analysis of the UAV relay coverage in mobile ad-hoc network. *Appl. Mech. and Mat*. 2014; 577: 879-883.
[19] Bashir E-J, Steele R. Cellular communications using aerial platforms. *IEEE Trans. on Veh. Technol*. 2001; 50(3): 686-700.
[20] Perumal S, Baras J S, Graf C J, et al. *Aerial platform placement algorithms to satisfy connectivity, capacity and survivability constraints in wireless ad-hoc networks*. IEEE Mil. Communication. Conf. 2008: 1-7.
[21] Boyer J, Falconer DD, Yanikomeroglu H. Multihop diversity in wireless relaying channel. *IEEE Trans. Commun*. 2004; 52(10): 1820–1830.
[22] Lee IH, Kim D. Coverage extension and power allocation in dual-hop spacetime transmission with multiple antennas in each node. *IEEE Trans. Veh. Technol*. 2007; 56(6): 3524–3532.
[23] Laneman JN, Tse DNC, Wornell GW. Cooperative diversity in wireless networks: Efficient protocols and outage behavior. *IEEE Trans. Inf. Theory*. 2004; 50(12): 3062–3080.
[24] Paulraj A, Nabar R, Gore D. Introduction to space-time wireless communications. Cambridge, UK: Cambridge University Press. 2003.
[25] Grace D, Daly NE, Tozer TC, Burr AG, Pearce DAJ. Providing multimedia communications services from high altitude platforms. *Int. J. of Satell. Commun*. 2001; (19): 559-580.
[26] Xu H, Rappaport TS, Boyle RJ, Schaffner JH. Measurements and models for 38-GHz point-to-multipoint radiowave propagation. *IEEE J. on Sel. Areas in Commun*. 2000; 18: 310-321.
[27] Michailidis ET, Kanatas AG. *Capacity optimized line-of-sight HAP-MIMO channels for fixed wireless access*. Int. Workshop on Satell. and Space Commun. (IWSSC). 2009: 73-77.
[28] International Telecommunication Union (ITU). *Specific attenuation model for rain for use in prediction methods*. ITU-R P.838-1. Geneva, Switzerland. 1997.
[29] International Telecommunication Union (ITU). *Characteristics of precipitation for propagation modeling*. ITU-R P.837-4. Geneva, Switzerland. 2003.
[30] Salo J, El-Sallabi HM, Vainikainen P. The distribution of the product of independent Rayleigh random variables. *IEEE Trans. on Antennas and Propag*. 2006; 54(2): 639-643.
[31] The Wolfram Functions Site. Available from http://functions.wolfram.com
[32] Erceg V, Fortune SF, Ling J, Rustako AJ Jr, Valenzuela RA. Comparisons of a computer-based propagation prediction tool with experimental data collected in urban microcellular environments. *IEEE J. on Sel. Areas in Commun*. 1997; 15(4). 677–684.
[33] Mathai AM, Saxena RK. Generalized hypergeometric functions with applications in statistics and physical sciences. Berlin, Germany: Springer-Verlag. 1973.